

## Super-resolution in confocal scanning microscopy

This article has been downloaded from IOPscience. Please scroll down to see the full text article.

1987 Inverse Problems 3 195

(<http://iopscience.iop.org/0266-5611/3/2/006>)

View [the table of contents for this issue](#), or go to the [journal homepage](#) for more

Download details:

IP Address: 130.251.61.251

The article was downloaded on 21/04/2010 at 09:38

Please note that [terms and conditions apply](#).

## Super-resolution in confocal scanning microscopy

M Bertero†, P Brianzi‡ and E R Pike§

† Dipartimento di Fisica dell'Università and Istituto Nazionale di Fisica Nucleare, I-16146 Genova, Italy

‡ Istituto Matematico dell'Università, I-16132 Genova, Italy

§ King's College, London and Royal Signals and Radar Establishment, Great Malvern, Worcestershire WR14 3PS, UK

Received 4 April 1986, in final form 31 July 1986

**Abstract.** In a previous paper it was shown that the resolution of the type-II confocal scanning microscope may be improved by recording the full image and by inverting the data. In this paper we propose a numerical method which can be easily implemented and, in principle, applied to the practical problem. We show that by using a rather small number of data points on the image plane, it is possible to obtain the improvement in resolution (by a factor of two) predicted in our previous analysis.

### 1. Introduction

In confocal scanning light microscopy a plane wave front is focused on the object plane by a lens, which we may call the illumination lens, and an image is formed by a second lens, the collector lens [1–3]. Then, if  $f(y)$  is the complex amplitude transmission of the object and if the illumination and collector lenses have the same point spread function  $S(x)$ , the full image formed by the microscope is

$$g(x) = \int S(x-y)S(y)f(y) dy \quad (1.1)$$

where magnification factors have been omitted. A translation of the specimen by  $\xi$  gives a new image

$$g(\xi, x) = \int S(x-y)S(y)f(y + \xi) dy. \quad (1.2)$$

In the type-II (scanning) microscope [1–3], the image is recorded at  $x=0$ , say  $G(\xi) = g(\xi, 0)$ , and from equation (1.2), ignoring detector integration and assuming an even point spread function, it follows that

$$G(\xi) = \int S^2(\xi-y)f(y) dy. \quad (1.3)$$

Thus the amplitude point spread function of the type-II microscope is the same as the intensity point spread function of an incoherently illuminated ordinary (type I) microscope.

In [4] it was shown that the resolution of the type-II microscope may be improved if, at each scanning position  $\xi$ , the full image  $g(\xi, x)$  is recorded and the integral equation (1.2) is

solved to estimate  $f(\xi)$ . For this purpose singular function expansions were used [6] and a detailed investigation of the one-dimensional problem was performed assuming uniformly filled lenses. In such a case, taking the Rayleigh distance associated with the lens as the unit of length, equation (1.1) becomes

$$g(x) = \int_{-\infty}^{+\infty} \text{sinc}(x-y) \text{sinc}(y) f(y) dy \tag{1.4}$$

where

$$\text{sinc}(x) = \frac{\sin(\pi x)}{\pi x}. \tag{1.5}$$

In [4] the singular system of the integral operator described by equation (1.4) was determined numerically. A beautiful and new result, proved recently by Gori and Guattari [5], shows that the singular functions of such an operator can be expressed analytically in terms of sinc functions and have a close connection with the sampling theorem. We first review this recent work.

Let  $A$  be the integral operator defined by

$$(Af)(x) = \int_{-\infty}^{+\infty} \text{sinc}(x-y) \text{sinc}(y) f(y) dy. \tag{1.6}$$

Then the null space of  $A$ , i.e. the set of the functions  $f(y)$  which produce a zero image ('invisible' objects), contains all the functions  $f(y)$  whose Fourier transform is zero over the interval  $[-2\pi, 2\pi]$  and also the band-limited functions, with bandwidth  $2\pi$ , which are zero at the sampling points  $y=0$  and  $y_n = \pm(n + \frac{1}{2})$  with  $n = 1, 2, 3, \dots$ . It follows that the orthogonal complement of the null space of  $A$ , i.e. the set of the 'visible' or fully 'transmitted' objects, is just the set of the band-limited functions, with bandwidth  $2\pi$  (twice the bandwidth of the lens), which are zero at the sampling points  $y_n = \pm n$  with  $n = 1, 2, 3, \dots$ . Notice that these are precisely the zeros of the illuminating profile  $P(y) = \text{sinc}(y)$ .

The singular system  $\{\alpha_k; u_k, v_k\}_{k=0}^{+\infty}$  of the operator  $A$  is the set of the solutions of the coupled equations

$$Au_k = \alpha_k v_k \quad A^* v_k = \alpha_k u_k \tag{1.7}$$

where  $A^*$  is the adjoint of  $A$ . The singular functions  $u_k$  form an orthonormal basis in the subspace of the 'transmitted' objects while the singular functions  $v_k$  form a basis in the space of the band-limited images  $g(x)$  with bandwidth  $\pi$ . The  $u_k$  and the associated  $v_k$  are alternatively even and odd. The singular values associated with the odd singular functions have the simple expression [5]

$$\alpha_k = \alpha_{2m+1} = \frac{\sqrt{2}}{\pi(2m+1)} \quad m = 0, 1, 2, \dots \tag{1.8}$$

while the singular values associated with the even singular functions are given by

$$\alpha_k = \alpha_{2m} = \sqrt{2}/\beta_m \quad m = 0, 1, 2, \dots \tag{1.9}$$

where the  $\beta_m$  are the solutions of the equation

$$\tan(\beta/2) = 2/\beta \tag{1.10}$$

and therefore  $\beta_m \sim 2\pi m, m \rightarrow \infty$ .

Finally the odd singular functions have the simple expression

$$v_{2m+1}(x) = \frac{1}{\sqrt{2}} \left[ \operatorname{sinc} \left( x - \frac{2m+1}{2} \right) - \operatorname{sinc} \left( x + \frac{2m+1}{2} \right) \right] \quad (1.11)$$

$$u_{2m+1}(x) = \operatorname{sinc} \left[ 2 \left( x - \frac{2m+1}{2} \right) \right] - \operatorname{sinc} \left[ 2 \left( x + \frac{2m+1}{2} \right) \right], \quad (1.12)$$

while the even singular functions are given by

$$v_{2m}(x) = N_m \left[ \operatorname{sinc} \left( x - \frac{\beta_m}{2\pi} \right) - \operatorname{sinc} \left( x + \frac{\beta_m}{2\pi} \right) \right] \quad (1.13)$$

$$u_{2m}(x) = \frac{1}{\alpha_{2m}} \operatorname{sinc}(x) v_{2m}(x) \simeq 2m \frac{\sin^2(\pi x)}{\pi^2(x^2 - m^2)}. \quad (1.14)$$

In (1.13)  $N_m$  is a normalisation constant and in (1.14) the behaviour of  $u_{2m}(x)$ , for large  $m$ , is also given. From equations (1.11)–(1.14) the connection between singular function expansions and the sampling theorem may be easily seen. These new results clearly simplify the use of the singular system expansions proposed for scanning microscopy in reference [4].

The transmitted part of the solution of equation (1.4) can be expressed in terms of the singular functions. The result is

$$f^{(t)}(y) = \sum_{k=0}^{+\infty} \frac{1}{\alpha_k} (g, v_k) u_k(y) \quad (1.15)$$

where

$$(g, v_k) = \int_{-\infty}^{+\infty} g(x) v_k(x) dx. \quad (1.16)$$

This solution is ill-posed since the  $\alpha_k$  tend to zero when  $k \rightarrow \infty$  and therefore, in the case of noisy data, the series must be truncated in order to have meaningful results.

The usual criterion is to take only those terms which correspond to singular values  $\alpha_k$  greater than the inverse of the given signal-to-noise ratio. This criterion might require a rather large number of terms in (1.15), since the singular values  $\alpha_k$  tend to zero rather slowly. However, as follows from the connection between singular function expansions and the sampling theorem pointed out above, only the very first terms in (1.15) contribute to the restoration of  $f^{(t)}(y)$  in the region corresponding to the central lobe of the illuminating profile. The other terms mainly contribute to the restoration of  $f^{(t)}(y)$  outside this region but this restoration is not required because the outer regions can be reached by the scanning procedure.

This remark implies that the truncation of the expansion (1.15) is not dictated by the signal-to-noise ratio but by the requirement of reconstructing  $f^{(t)}(y)$  only inside the central lobe of the illuminating profile. By inspection of the singular functions  $u_k(y)$ , which are plotted in [4], one can argue that at most seven terms in (1.15) contribute to the central region and that even five terms would provide a satisfactory approximation. Notice that  $\alpha_0/\alpha_4 = 7.5$  and  $\alpha_0/\alpha_6 = 11.1$ ; for both cases the restoration of  $f^{(t)}(y)$  is a quite well conditioned problem.

The previous analysis applies to the case where the function  $g(x)$  is known everywhere. In practice we know only a finite set of values of  $g(x)$ . In these circumstances one can apply the general method formulated in [6] and already used in [4]. However this method requires the computation of the Gram matrix associated with the problem and, in the

present case, this is a rather heavy numerical problem. For this reason we prefer an approximate treatment based on the use of the appropriate sampling expansions for the functions  $g(x)$  and  $f(y)$  in equation (1.4). In § 2 we outline this method and we show, by numerical computation, that using 5 or 7 sampling points (at the Rayleigh distance) in the image plane it is possible to have fairly good approximations of the first 5 or 7 singular values respectively.

In § 3 we discuss a simulation of a discrete scanning procedure in one dimension. The distance between adjacent scanning positions is just one half of the Rayleigh distance, and for each position the image is recorded at five points sampled at the Rayleigh distance. For inversion the singular system computed in § 2 is used. Two different restoration schemes are considered. The first one restores the central value of  $f^{(l)}(y)$  at each scanning position while the second restores  $f^{(l)}(y)$  at the three sampling points internal to the central lobe of the illuminating profile and uses the arithmetic mean of the values obtained in adjacent scanning positions as an estimation of the central value. In both cases the restored central values are interpolated by means of sinc functions with bandwidth  $2\pi$ . We find, as is to be expected, that the second method produces better statistics than the first one.

Finally, in § 4 we discuss the 2D problem in the case of square pupils since in such a case the singular functions are simply obtained as tensor products of the singular functions of the 1D problem. The extension to the 2D case of the scanning procedure investigated in § 3 is obvious. Numerical simulations can be performed using the 1D singular system computed by means of the method presented in § 2. For simplicity only the method of reconstruction of  $f^{(l)}$  at the central point is calculated and it is found that this provides quite good results.

## 2. Singular system and sampling expansion in the one-dimensional problem with discrete data

Assume that  $g$  is sampled at the Nyquist rate and therefore measured at the sampling points  $x_n = n$  ( $n = 0, \pm 1, \dots, \pm N$ ). Then equation (1.4) can be written in the form (see [6])

$$g(n) = (f, \varphi_n) \quad (2.1)$$

where the scalar product is that of  $L^2(-\infty, +\infty)$  and

$$\varphi_n(y) = \text{sinc}(y-n) \text{sinc}(y). \quad (2.2)$$

As shown in [6], the singular system of the problem with discrete data can be determined by diagonalising the Gram matrix of the functions  $\varphi_n$ , i.e.

$$\mathbf{G}_{nm} = (\varphi_n, \varphi_m) = \int_{-\infty}^{+\infty} \text{sinc}(y-n) \text{sinc}^2(y) \text{sinc}(y-m) dy, \quad (2.3)$$

and therefore the method requires the numerical computation of some improper integrals.

A much simpler approach can be obtained by using the sampling expansions of  $g(x)$  and  $f^{(l)}(y)$  (the ‘transmitted’ part of  $f(y)$ ) and in such a way transforming the integral equation (1.4) into a (infinite dimensional) matrix equation.

If  $g(x)$  is given by equation (1.4), i.e. if  $g(x)$  is a noise-free image, then  $g(x)$  is band-limited, with bandwidth  $\pi$ , and can be represented by the sampling expansion

$$g(x) = \sum_{n=-\infty}^{+\infty} b_n \text{sinc}(x-n) \quad (2.4)$$

where  $b_n = g(n)$ . On the other hand the transmitted part of  $f(y)$ , i.e. the part of  $f(y)$  which can be determined from the data, is a band-limited function which has a bandwidth  $2\pi$  and is zero at the sampling points  $y_n = n$  ( $n = \pm 1, \pm 2, \dots$ ). It follows that  $f^{(t)}(y)$  can be represented as follows

$$f^{(t)}(y) = \sum_{m=-\infty}^{-1} a_m \operatorname{sinc}[2(y - m - \frac{1}{2})] + a_0 \operatorname{sinc}(2y) + \sum_{m=1}^{+\infty} a_m \operatorname{sinc}[2(y - m + \frac{1}{2})]. \tag{2.5}$$

In figure 1 we give, for comparison, the sampling schemes for  $g(x)$  and  $f^{(t)}(y)$  and we also plot the illuminating profile. It is clearly seen that the three sampling points inside the central lobe are spaced by half the Rayleigh distance and this fact is the origin of the improvement by a factor of two in resolution which can be obtained by means of the scanning procedure. Outside the central lobe the resolution is exactly equal to the Rayleigh distance.

If we substitute the expansions (2.4) and (2.5) into equation (1.4) we obtain the equation

$$b_n = \sum_{m=-\infty}^{+\infty} A_{nm} a_m \quad n = 0, \pm 1, \pm 2 \dots \tag{2.6}$$

where

$$A_{nm} = \int_{-\infty}^{+\infty} \operatorname{sinc}(y - n) \operatorname{sinc}(y) \operatorname{sinc}[2(y - m - \frac{1}{2})] dy \quad m < 0 \tag{2.7}$$

$$A_{n0} = \int_{-\infty}^{+\infty} \operatorname{sinc}(y - n) \operatorname{sinc}(y) \operatorname{sinc}(2y) dy \tag{2.8}$$

$$A_{nm} = \int_{-\infty}^{+\infty} \operatorname{sinc}(y - n) \operatorname{sinc}(y) \operatorname{sinc}[2(y - m + \frac{1}{2})] dy \quad m > 0. \tag{2.9}$$

Equation (2.6) is exactly equivalent to equation (1.4) as far as the determination of the transmitted part of  $f(y)$  is concerned. Indeed the operator defined by the infinite dimensional matrix  $A_{nm}$  is invertible while the integral operator (1.6) is not.

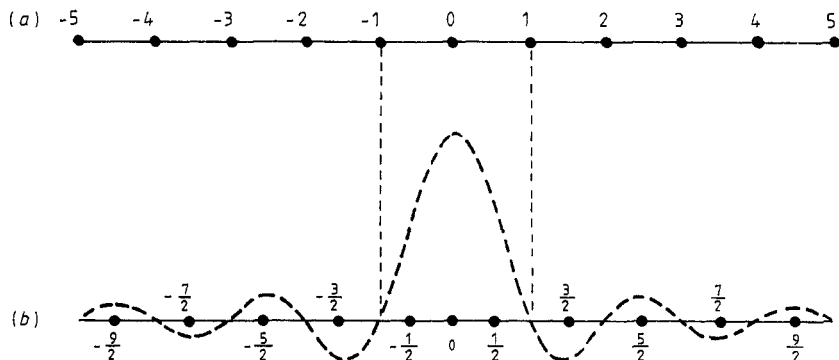


**Figure 1.** Comparison of the sampling scheme for (a) the image and (b) the object. The illumination profile is also indicated.

The integrals in the equations (2.7)–(2.9) can be computed analytically using the projection properties of the function  $\text{sinc}(2x)$  (technically  $\text{sinc}(2x)$  is the reproducing kernel in the space of band-limited functions with bandwidth  $2\pi$ ). The result is

$$A_{nm} = \frac{(-1)^n}{2\pi^2(m + \frac{1}{2})(m - n + \frac{1}{2})} \quad m < 0 \tag{2.10}$$

$$A_{n0} = \frac{1}{2} \delta_{n0} \tag{2.11}$$

$$A_{nm} = \frac{(-1)^n}{2\pi^2(m - \frac{1}{2})(m - n - \frac{1}{2})} \quad m > 0 \tag{2.12}$$

where  $\delta_{nm}$  is the usual Kronecker symbol.

Returning to the problem with discrete data we restrict the index  $n$  to the values  $n = 0, \pm 1, \dots, \pm N$  while the index  $m$ , in principle, runs from  $-\infty$  to  $+\infty$ . Obviously, for numerical computation we must limit also the index  $m$ , say to the values  $m = 0, \pm 1, \dots, \pm M$  but we can take  $M$  large enough in order to have no significant variation, on increasing  $M$ , in the computed singular values.

The problem now is the standard one of the numerical computation of the singular system of a matrix  $\mathbf{A}$ ,  $(2N + 1) \times (2M + 1)$ , given by equations (2.10)–(2.12). Obviously we can always assume  $N \leq M$ . Then, if we denote by  $\{\alpha_k; \mathbf{u}_k, \mathbf{v}_k\}_{k=0}^{2N}$  the singular system of  $\mathbf{A}$  (we omit  $N$  and  $M$  for simplicity) we know that, when  $N, M \rightarrow \infty$  the singular values of  $\mathbf{A}$  converge to the singular values of  $A$ , equation (1.6) [4]. Furthermore, if we introduce the functions

$$u_k(y) = \sum_{m=-M}^{-1} (u_k)_m \text{sinc}[2(y - m - \frac{1}{2})] + (u_k)_0 \text{sinc}(2y) + \sum_{m=1}^M (u_k)_m \text{sinc}[2(y - m + \frac{1}{2})] \tag{2.13}$$

they also converge to the singular functions of the operator (1.6) when  $N, M \rightarrow \infty$  (the convergence is in the norm of  $L^2(-\infty, +\infty)$ ).

We make a technical remark before presenting the numerical results. For the question of normalisation, in the space of the object vectors we introduce the norm

$$\|\mathbf{a}\|_0^2 = \frac{1}{2} \sum_{m=-M}^M |a_m|^2 \tag{2.14}$$

while in the image space we put

$$\|\mathbf{b}\|_1^2 = \sum_{n=-N}^N |b_n|^2. \tag{2.15}$$

Then it follows that the adjoint matrix  $\mathbf{A}^*$  is given by

$$\mathbf{A}_{mn}^* = 2\mathbf{A}_{nm}. \tag{2.16}$$

By fixing the number of image points  $N' = 2N + 1$ , we have computed the singular values of the matrix  $\mathbf{A}$  for various values of the number of object points  $M' = 2M + 1$ . It is not difficult to recognise that for fixed  $N'$ , the singular values are increasing functions of  $M'$ , so that we always find lower bounds of the singular values of the problem with discrete data detailed at the beginning of this section. In table 1 we give an example of the behaviour of the singular values as a function of  $M'$ , for a fixed number of data points  $N = 5$ .

**Table 1.** Behaviour of the singular values of the problem with five data points as a function of the number of sampling points in the object.

$k$	$M' = 5$	$M' = 11$	$M' = 17$	$M' = 25$
0	0.821687	0.821797	0.821805	0.821807
1	0.412786	0.413810	0.413815	0.413815
2	0.204498	0.206202	0.206304	0.206327
3	0.129356	0.136859	0.136872	0.136873
4	0.084262	0.109424	0.109697	0.109751

**Table 2.** Comparison between the singular values of the problem with infinite data (first column), as derived from the paper of Gori and Guattari [5], and the singular values of various problems with discrete data.

$k$	$N' = \infty, M' = \infty$	$N' = 17, M' = 17$	$N' = 7, M' = 17$	$N' = 5, M' = 17$
0	0.821898	0.821894	0.821862	0.821805
1	0.450158	0.439415	0.424153	0.413815
2	0.206417	0.206388	0.206357	0.206304
3	0.150053	0.146409	0.141044	0.136872
4	0.109845	0.109784	0.109755	0.109697
5	0.0900316	0.0877635	0.0840425	—
6	0.0742032	0.0741063	0.0740587	—
7	0.0643083	0.0625885	—	—
8	0.0559186	0.0557775	—	—

A remarkable property is that even with a rather small number of data points it is possible to obtain a good approximation of the largest singular values of the problem. This property is shown in table 2 (notice however that the approximation is better in the case of the 'even' singular values) and this is quite promising for the potential practical applications of this procedure. It implies that, for each scanning position, one needs to measure only a small number of sample values of the image.

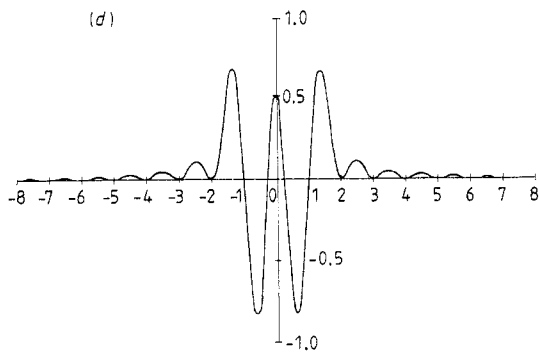
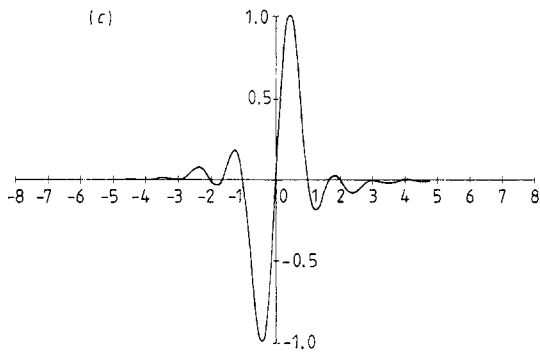
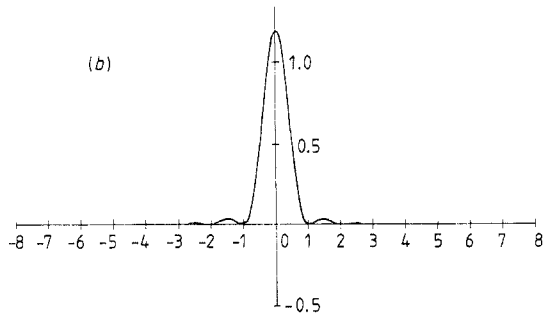
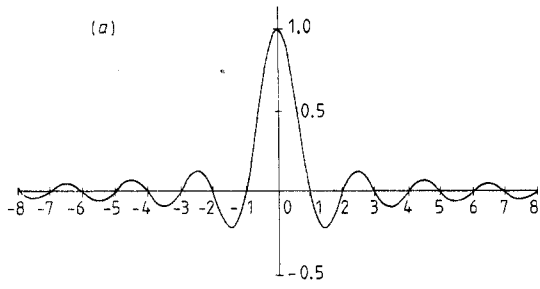
Finally we give in figure 2 the first five singular functions  $u_k(y)$  of the problem with five data points. These functions have been computed, in the case  $M' = 25$ , using equation (2.13), and they provide a good approximation of the functions given by equations (1.12) and (1.14).

### 3. Simulation of the scanning procedure in one dimension

From the results derived in [4, 5] it follows that, by combining scanning and inversion, it is possible to determine the projection of the object  $f(y)$  on the subspace of the band-limited functions with bandwidth  $2\pi$ , which is twice the bandwidth of the lenses. Since the component of  $f(y)$  orthogonal to this subspace is invisible, or, in other words, the Fourier components of  $f(y)$  out of the interval  $[-2\pi, 2\pi]$  are lost, we can assume that  $f(y)$  itself is band-limited, so that it can be represented by the sampling expansion

$$f(y) = \sum_{p=-\infty}^{+\infty} c_p \operatorname{sinc}[2(y - \frac{1}{2}p)] \quad (3.1)$$

where  $c_p = f(\frac{1}{2}p)$ .



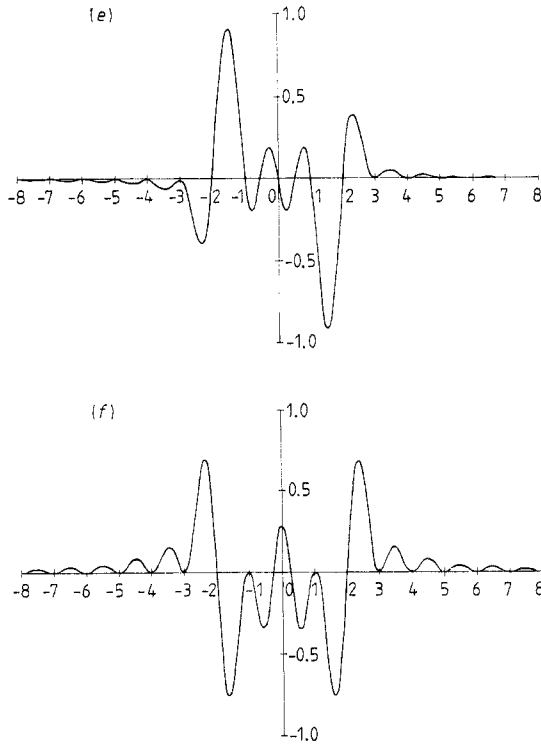


**Figure 2.** Singular functions for the problem with 5 data points using 25 sampling points in object space: (a) the illuminating profile, (b)  $u_0$ , (c)  $u_1$ , (d)  $u_2$ , (e)  $u_3$ , (f)  $u_4$ .

In the absence of noise, using the inversion formula (1.15) applied to the full image of  $f(y)$ , one can recover the coefficients  $c_0, c_{\pm 1}, c_{\pm 3}$  etc of the expansion (3.1). The missed coefficients  $c_{\pm 2}, c_{\pm 4}$  etc can be recovered by applying again the inversion formula (1.15) to the full image of  $f(y + \frac{1}{2})$ . Therefore, in this ideal case, two scanning positions are sufficient to recover completely the object  $f(y)$ .

However, we know that, in the presence of noise, the expansion (1.15) must be truncated. As a consequence, for a given position of the specimen,  $f(y)$  can be recovered only over a finite region and several scanning positions are required to obtain a complete reconstruction of  $f(y)$ .

In the following we assume that the distance between two adjacent scanning positions is  $\frac{1}{2}$ , i.e. half the Rayleigh distance. Furthermore it is quite natural to assume that  $f(y)$  has approximately a finite spatial extent, so that only a finite number of coefficients, say  $c_1, c_2, \dots, c_p$  are different from zero in the expansion (3.1).

In order to recover such a function we consider a scan consisting of exactly  $P$  scanning positions. At the position  $s$ , the object is

$$f_s(y) = f(y + \frac{1}{2}s) \quad s = 1, 2, \dots, P \tag{3.2}$$

and it can be decomposed into a visible and an invisible component. The transmitted component is determined by comparing the expansion of  $f_s(y)$  derived from (3.1) with the expansion (2.5). It follows that the coefficients  $a_{m,s}$  of  $f_s^{(0)}(y)$  are given by

$$a_{0,s} = c_s \quad a_{\pm m,s} = c_{s \pm (2m-1)} \quad (m = 1, 2, 3 \dots) \tag{3.3}$$

where  $c_p = 0$  if  $p < 1$  or  $p > P$ . Finally the coefficients  $b_{n,s}$ , in the expansion (2.4) for the image  $g_s(x)$  of  $f_s^{(0)}(y)$ , can be determined by means of equation (2.6). Notice that the matrix  $A_{nm}$  does not depend on the scanning position because, as specified in the introduction, we consider a scan of the specimen with a fixed illumination and imaging system.

Thus, the plan of a first part of a computer simulation experiment is the following: (a) specify the object  $f(y)$  by giving a set of coefficients  $c_p$  ( $p = 1, \dots, P$ ); (b) compute for each scanning position the image coefficients. If for each scanning position we compute  $2N + 1$  image points, then the final result is a set of  $P$   $(2N + 1)$ -dimensional vectors  $\mathbf{b}^{(1)}, \mathbf{b}^{(2)}, \dots, \mathbf{b}^{(P)}$ , whose components are given by  $(\mathbf{b}^{(s)})_n = b_{n,s}$ . The components of these vectors, if desired, may be contaminated by noise using sequences of random numbers. This point, however, is not essential because, as already remarked in the introduction, our reconstruction algorithms will be very well conditioned.

Assume that the singular system  $\{\alpha_k; \mathbf{u}_k, \mathbf{v}_k\}_{k=0}^{2N}$  of the  $(2N + 1) \times (2M + 1)$  matrix  $\mathbf{A}$  has been stored ( $N < M$ ). Then the reconstructed object vector corresponding to the scanning position  $s$  can be easily computed by means of the formula

$$\tilde{\mathbf{a}}^{(s)} = \sum_{k=0}^{2N} \frac{1}{\alpha_k} (\mathbf{b}^{(s)}, \mathbf{v}_k)_1 \mathbf{u}_k \quad (3.4)$$

the scalar product being defined by equation (2.15). The  $m$ th component of  $\tilde{\mathbf{a}}^{(s)}$ , i.e.  $(\tilde{\mathbf{a}}^{(s)})_m = \tilde{a}_{m,s}$  is the reconstructed value of the coefficient  $a_{m,s}$  of the object  $f_s^{(0)}(y)$ . In this way, for each position  $s$ , we can have  $2M + 1$  coefficients, which are values of the reconstructed object at certain sets of  $M + 1$  sampling points. It follows that, for a given sampling point  $p$ , the value of the recovered object  $f(y)$  at  $p$  can be obtained several times, namely for all the values of  $s$  and  $m$  such that  $s \pm (2m - 1) = p$  (see equation (3.3)). Due to the noise and to the approximate inversion method, these values will not exactly coincide. For this reason, we have considered two methods for estimating the coefficients  $c_p$  in the expansion (3.1) of  $f(y)$ . We denote by  $\tilde{c}_p$  the estimate of  $c_p$  and by  $\tilde{f}(y)$  the estimate of the object obtained by interpolating the  $\tilde{c}_p$  by means of sinc functions as in (3.1).

*Method 1.* We compute only the zero component of  $\tilde{\mathbf{a}}^{(p)}$  and we take this value as an estimate of  $\tilde{c}_p$ , i.e.

$$\tilde{c}_p = (\tilde{\mathbf{a}}^{(p)})_0 \quad p = 1, \dots, P. \quad (3.5)$$

This method is equivalent to the procedure, considered in [4], of reconstructing only the central point of the object  $f_s(y)$ .

In order to find the impulse response of this procedure, assume noise-free data in equation (3.4), i.e.  $\mathbf{b}^{(s)} = \mathbf{A}\mathbf{a}^{(s)}$ ; then we have

$$\begin{aligned} \tilde{c}_p &= \sum_{k=0}^{2N} \frac{1}{\alpha_k} (\mathbf{a}^{(p)}, \mathbf{A}^* \mathbf{v}_k)_0 (\mathbf{u}_k)_0 \\ &= \sum_{k=0}^{2N} (\mathbf{a}^{(p)}, \mathbf{u}_k)_0 (\mathbf{u}_k)_0 \\ &= \sum_{k=0}^{2N} u_k(0) \int_{-\infty}^{+\infty} f(\xi + \frac{1}{2}p) u_k(\xi) d\xi \\ &= \sum_{k=0}^{2N} u_k(0) \int_{-\infty}^{+\infty} u_k(\xi - \frac{1}{2}p) f(\xi) d\xi \end{aligned} \quad (3.6)$$

where  $u_k(\xi)$  is the singular function defined in equation (2.13). Now, if we interpolate the reconstructed sampled values  $\tilde{c}_p$  by means of equation (3.1) and if we use the following approximate relation

$$\sum_p \text{sinc}[2(y - \frac{1}{2}p)]u_k(\xi - \frac{1}{2}p) = u_k(\xi - y) \tag{3.7}$$

we find that

$$\tilde{f}(y) = \int_{-\infty}^{+\infty} A_1(y - \xi)f(\xi) d\xi, \tag{3.8}$$

where

$$A_1(x) = \sum_{k=0}^{2N} u_k(0)u_k(x). \tag{3.9}$$

Equation (3.7) is not exact but approximate, because we have only a finite number of terms on the RHS. However, the approximation is good when  $P$  is large.

Equations (3.9), (3.10) are just the equivalent of equations (7.11), (7.12) derived in [4] in the case of continuous data. Now, in the case  $N \rightarrow \infty, M \rightarrow \infty$ , the limit of equation (3.9) is

$$A_1^\infty(x) = \sum_{k=0}^{+\infty} u_k(0)u_k(x) \tag{3.10}$$

where the  $u_k$  are the singular functions of the operator (1.6). In [5], the following identity was derived

$$\sum_{k=0}^{+\infty} u_k(x)u_k(y) = 2[\text{sinc}(2x) \text{sinc}(2y) + \sin(\pi x) \sin(\pi y) \text{sinc}(x - y)] \tag{3.11}$$

and therefore we obtain

$$A_1^\infty(x) = \frac{\sin(2\pi x)}{\pi x} \tag{3.12}$$

which is just the limiting case derived in [4]. For finite  $N$ , from the computations performed in [4] we expect that  $A_1(x)$ , equation (3.9), has a rather large zero-frequency component, which could introduce distortions in the reconstruction of  $f(y)$ .

*Method 2.* For each scanning position  $s$  we reconstruct the three sampling values of  $f(y + s/2)$  interior to the illuminating profile, i.e.  $\tilde{a}_{-1}^{(s)}, \tilde{a}_0^{(s)}, \tilde{a}_1^{(s)}$  and we take as an estimate of  $c_p$  the arithmetic mean of these values obtained in adjacent scanning positions. In such a way we have

$$\tilde{c}_p = \frac{1}{3}(\tilde{a}_1^{(p-1)} + \tilde{a}_0^{(p)} + \tilde{a}_{-1}^{(p+1)}). \tag{3.13}$$

In [4] this procedure was considered in the case where the average is made over a large number of reconstructed values and it was found that the corresponding impulse response has a zero-frequency component which is too small. Therefore one can hope that the choice (3.13) is a good compromise between the estimation on only one point and the estimation over a large number of points.

By computations similar to those performed in equation (3.6) it follows that the impulse response of this method is

$$A_2(x) = \frac{1}{3} \sum_{k=0}^{2N} [u_k(-\frac{1}{2})u_k(x-\frac{1}{2}) + u_k(0)u_k(x) + u_k(\frac{1}{2})u_k(x+\frac{1}{2})]. \quad (3.14)$$

Using equation (3.11) again it should be possible to compute the limit of  $A_2(x)$  when the number of points tends to infinity. However, this limit is not interesting since we expect that this method works well only when we have a small number of data points.

In figure 3 we compare the ideal impulse response  $A_1^\infty(x)$  with  $A_1(x)$  and  $A_2(x)$  both computed in the case of five data points. We notice that  $A_1(x)$  has rather large positive sidelobes and that  $A_2(x)$  appears to be a much better approximation of  $A_1^\infty(x)$ .

Both methods can be easily implemented on desk computers. To demonstrate the capabilities of the different inversion procedures using various approximate singular systems we present the results obtained with one example where  $P=25$ .

In table 3 we give the values of the 25 simulation sampling coefficients  $c_p$  and of the reconstructed coefficients  $\tilde{c}_p$  given by equation (3.5) or (3.13), both in the case  $N'=17$ ,  $M'=17$  (using 11 singular functions) and in the case  $N'=5$ ,  $M'=25$  (using 5 singular functions). The reconstructed values obtained by method 1 are systematically higher than

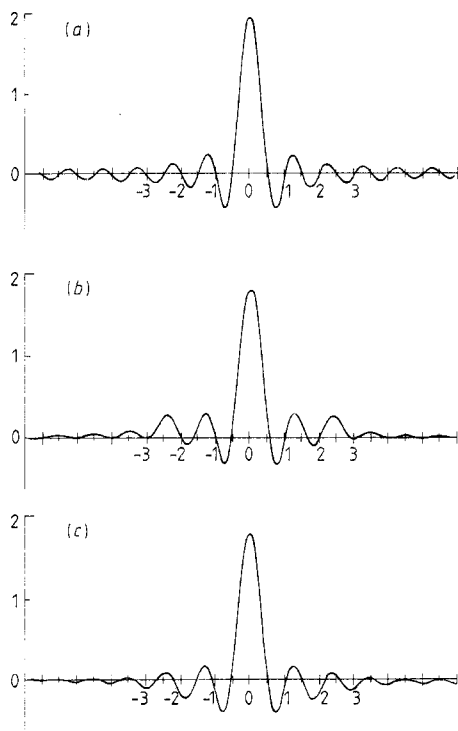


**Figure 3.** Comparison of (a) the impulse response function  $A_1^\infty(x)$  of equation (3.12), (b) the impulse response function  $A_1(x)$  for the case of five data points, and (c) the impulse response function  $A_2(x)$ , again in the case of five data points.

**Table 3.** Comparison of the sampling coefficients  $c_p$  with the reconstructed coefficients  $\tilde{c}_p$  obtained using the two methods considered in this section and two different approximations of the singular system. In the case  $N' = 17, M' = 17$ , 11 singular functions have been used while 5 singular functions have been used in the other case.

$p$	$c_p$	$\tilde{c}_p(N' = 17, M' = 17)$		$\tilde{c}_p(N' = 5, M' = 25)$	
		Method 1	Method 2	Method 1	Method 2
1	0	0.112	-0.018	0.215	0.018
2	0	0.157	0.008	0.229	0.024
3	0.2	0.341	0.138	0.394	0.122
4	0.5	0.667	0.454	0.671	0.441
5	0.8	0.963	0.753	0.922	0.714
6	1	1.134	0.935	1.223	0.983
7	0.8	0.967	0.764	0.934	0.673
8	0.5	0.640	0.435	0.744	0.444
9	0	0.164	-0.042	0.252	-0.122
10	0	0.147	-0.048	0.349	-0.053
11	1	1.123	0.942	1.261	0.846
12	0	0.147	-0.045	0.383	-0.060
13	0	0.153	-0.050	0.341	-0.108
14	0	0.153	-0.052	0.276	-0.106
15	0.3	0.450	0.247	0.565	0.198
16	0.5	0.653	0.450	0.754	0.435
17	0.9	1.051	0.847	1.049	0.833
18	1	1.158	0.942	1.114	0.919
19	0.2	0.380	0.155	0.387	0.179
20	0.8	0.953	0.741	0.923	0.693
21	0.1	0.249	0.051	0.322	0.064
22	0	0.143	-0.041	0.189	-0.099
23	0	0.118	-0.060	0.239	-0.011
24	0	0.155	-0.025	0.108	-0.010
25	0	0.113	-0.016	0.178	0.047

the true coefficients  $c_p$ . This effect is due to the large zero-frequency component of the impulse response function of method 1 (see [4]). It also appears from table 3 that the approximation provided by method 2 is considerably better than that provided by method 1.

In figure 4 we plot the interpolations of the various sets of coefficients given in table 3, except the case  $N' = 17, M' = 17$ , method 2, in which case the plot of the reconstructed function does not show appreciable variations with respect to the true function. We also give, for comparison, the images provided by the usual microscope and by the type-II scanning microscope.

In the case of the usual microscope, the image of the function (3.1) is

$$f_1(x) = \int_{-\infty}^{+\infty} \text{sinc}(x-y)f(y) dy = \frac{1}{2} \sum_p c_p \text{sinc}(x - \frac{1}{2}p) \tag{3.15}$$

(see figure 4(b)) while in the case of the type-II scanning microscope, the image is [4]

$$f_2(x) = \int_{-\infty}^{+\infty} \text{sinc}^2(x-y)f(y) dy = \frac{1}{2} \sum_p c_p \text{sinc}^2(x - \frac{1}{2}p) \tag{3.16}$$

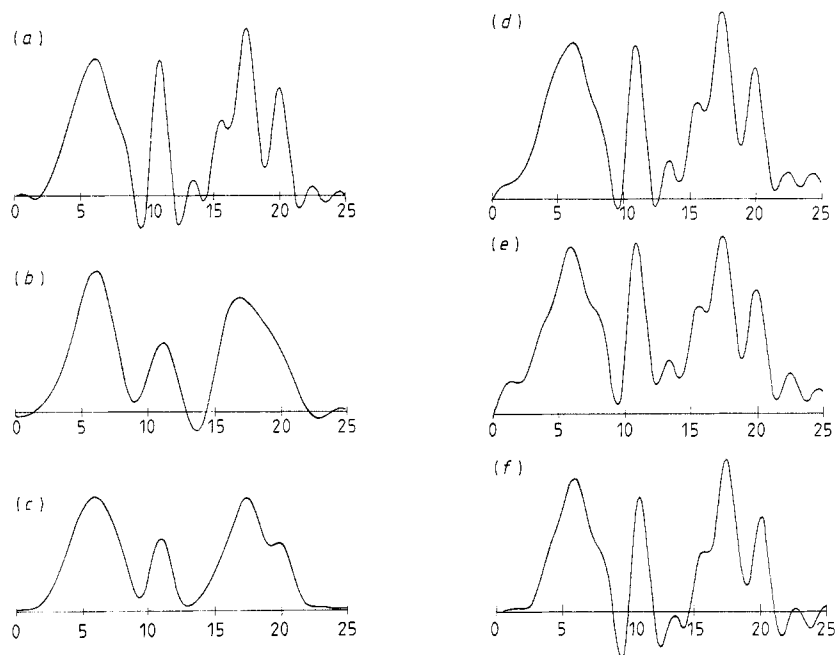


**Figure 4.** (a) The object corresponding to the coefficients  $c_p$  of table 3; (b) its image provided by the usual microscope; (c) its image provided by the type-II scanning microscope; (d) the reconstructed object obtained with 17 data points and 11 singular functions using method 1; (e) and (f) the reconstructed object obtained with five data points and five singular functions using method 1 (e) and method 2 (f).

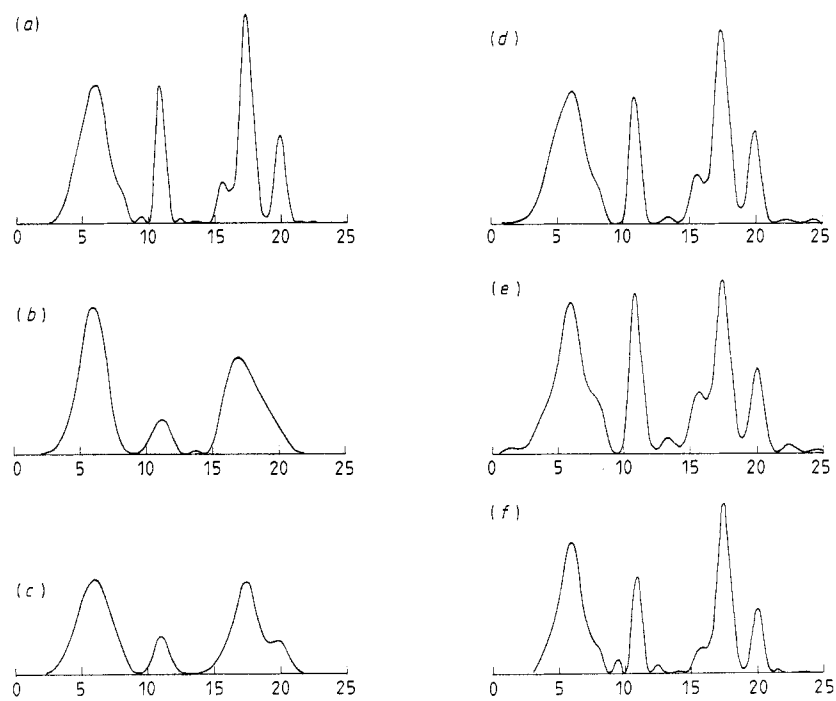


**Figure 5.** Plot of the intensities corresponding to the amplitudes plotted in figure 4.

(see figure 4(c)). The improvement obtained by means of our new inversion of the image is evident.

As we have said, the reconstructed object, in the case of 17 data points, 11 singular functions and method 2, is an excellent approximation of the true object. However, this is a quite large number of data points. Especially in the 2D case, considered in the next section, it is necessary to reduce the number of data points as far as possible. For this reason it is quite important that, using five data points and method 2, it is still possible to obtain a rather satisfactory reconstruction.

In figure 5 we plot the intensities corresponding to the amplitudes of figure 4 and remind the reader that our methods require phase as well as amplitude for the reconstruction of arbitrary asymmetric objects.

#### 4. The two-dimensional problem with square pupils

In the case of square pupils the solution of the two-dimensional (2D) problem can be reduced to the solution of the one-dimensional (1D) problem discussed in the previous sections. The integral equation is given by equation (1.1) with

$$S(\mathbf{x}) = \text{sinc}(x_1) \text{sinc}(x_2) \quad (4.1)$$

(here  $\mathbf{x} = \{x_1, x_2\}$ ). The Fourier transform of  $S(\mathbf{x})$ ,  $S(\boldsymbol{\omega})$ , is 1 over the square  $|\omega_1| \leq \pi$ ,  $|\omega_2| \leq \pi$  and 0 elsewhere. Therefore, in the absence of noise,  $g(\mathbf{x})$  is a band-limited function which can be recovered from its values at the points of a square lattice with cells of unit length (Rayleigh distance).

As in the one-dimensional case one can easily characterise the subspace of the 'invisible' objects, i.e. the objects which produce a zero image. The orthogonal complement of this subspace is the subspace of the 'transmitted' objects  $f^{(0)}(\mathbf{x})$ . It follows that  $f^{(0)}(\mathbf{x})$  is a band-limited function whose Fourier transform is zero out of the square  $|\omega_1| \leq 2\pi$ ,  $|\omega_2| \leq 2\pi$  and with sampling values different from zero only at the sampling points given in figure 6. Again, only at the centre of the object is an improvement of a factor of two with respect to the Rayleigh distance ( $R = 1$ ) obtained in the direction of both axes.

The transmitted part of the object can be expanded in the basis of the singular functions of the integral operator

$$(A^{(2)}f)(\mathbf{x}) = \int_{R^2} S(\mathbf{x}-\mathbf{y})S(\mathbf{y})f(\mathbf{y}) d\mathbf{y} \quad (4.2)$$

with  $S(\mathbf{x})$  given by equation (4.1) and the singular system of  $A^{(2)}$  is simply related to the singular system of the integral operator (1.6).

The singular values of  $A^{(2)}$  are given by all the possible products of the singular values of the operator  $A$

$$\alpha_{k,j} = \alpha_k \alpha_j \quad k, j = 0, 1, \dots \quad (4.3)$$

and the corresponding singular functions are the tensor products of the singular functions of  $A$ , equations (1.11)–(1.14).

$$u_{k,j}(\mathbf{x}) = u_k(x_1)u_j(x_2) \quad (4.4)$$

$$v_{k,j}(\mathbf{x}) = v_k(x_1)v_j(x_2). \quad (4.5)$$

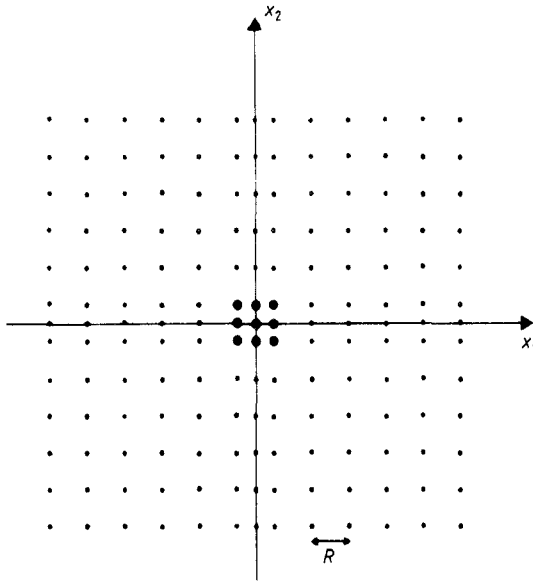


Figure 6. Sampling scheme for the ‘transmitted’ objects in the 2D case with square pupils.

It is obvious that the singular values  $\alpha_{k,j}$ , with  $k \neq j$ , have multiplicity 2 while the singular values  $\alpha_{j,j}$  have multiplicity 1.

The same relationship between the singular system of the 2D problem and the singular system of the 1D problem still holds true in the case of discrete data if, in the 2D problem, the data points form a square lattice with cells of unit length. Then one can use the 1D singular functions and singular vectors computed using the method of § 2.

The extension of the simulation of the scanning procedure to the 2D case is quite obvious. We assume that the object  $f(y)$  can be represented by the sampling expansion

$$f(y) = \sum_{p,q} c_{p,q} \text{sinc}[2(y_1 - \frac{1}{2}p)] \text{sinc}[2(y_2 - \frac{1}{2}p)] \tag{4.6}$$

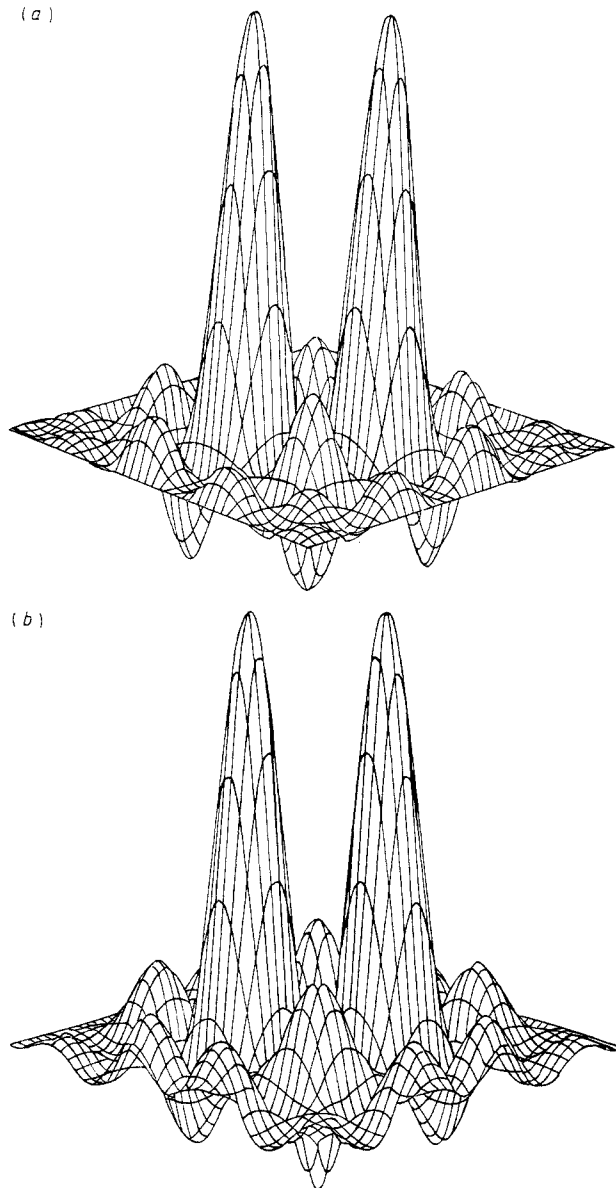
and that the scanning positions  $s$  form a square lattice with cells of dimensions  $\frac{1}{2}$ . For each scanning position one can compute  $f_s^{(t)}(y) = f^{(t)}(y + s)$  and the image vector. The inversion procedure is based on the obvious extension of equation (3.4).

Table 4. The restored values. Each entry has a true sampling value of zero except the two marked by † where the true sampling value is one.

0.023	0	0.017	0.124	0.016	0.078	0.018	0	0.025
0	0	0	0	0	0	0	0	0
0.017	0	0.013	0.078	0.012	0.069	0.013	0	0.018
0.124	0	0.078	0	0.069	0.857	0.069†	0	0.078
0.016	0	0.012	0.069	0.011	0.069	0.012	0	0.016
0.078	0	0.069	0.857†	0.069	0	0.078	0	0.124
0.018	0	0.013	0.069	0.012	0.078	0.013	0	0.017
0	0	0	0	0	0	0	0	0
0.025	0	0.018	0.078	0.016	0.124	0.017	0	0.023

In the case of method 1, we restore  $f_s^{(0)}(y)$  only for  $y=0$  and then interpolate the restored values by means of sinc functions as in equation (4.6). On the other hand the extension of method 2 corresponds first to restoring the values of  $f_s^{(0)}(y)$  at the nine sampling points internal to the central lobe (see figure 6) and then taking the arithmetic mean of the values obtained in adjacent scanning positions.

We have implemented only method 1, using the 1D singular system corresponding to  $N'=5$ ,  $M'=25$ . In this case, for each scanning position, we require 25 image points and



**Figure 7.** Plot of (a) the interpolated object whose sampling values are given in table 4, and (b) its restoration obtained using  $5 \times 5$  image points for each scanning position and method 1.

we use 25 singular functions for inversion. We have tested the method in a case with  $9 \times 9$  scanning positions. All the values of  $f(\mathbf{x})$  at the scanning positions were zero except two values on the diagonal (equal to one). In table 4 we give the sampling values of  $f(\mathbf{x})$  and the restored values. The approximation obtained by means of method 1 in the 2D case is much better than the approximation obtained by the same method in the 1D case. One can understand this by remarking that in the 2D case the positive sidelobes of the impulse response function are less important than in the 1D problem. In figure 7 we plot the interpolated object and the restored object corresponding to the sampling values of table 4.

The number of data points we use must be as small as possible for practical applications. Work is in progress aimed at reducing both the number of data points and the number of required singular functions. For this purpose we will investigate the use of non-uniform sampling distances in the image plane, which is suggested by recent results obtained by Luttrell in similar problems [7].

### Acknowledgment

This work has been partially supported by NATO Grant no 463/84.

### References

- [1] Sheppard C J R and Choudhury A 1977 Image formation in the scanning microscope *Opt. Acta* **24** 1051–73
- [2] Brakenhoff G J, Blom P and Barends P 1979 Confocal scanning light microscopy with high aperture immersion lenses *J. Microsc.* **117** 219–32
- [3] Wilson T and Sheppard C 1984 *Theory and Practice of Scanning Microscopy* (London: Academic)
- [4] Bertero M, De Mol C, Pike E R and Walker J G 1984 Resolution in diffraction-limited imaging: IV—The case of uncertain localisation or non-uniform illumination of the object *Opt. Acta.* **31** 923–46
- [5] Gori F and Guattari G 1985 Signal restoration for linear systems with weighted impulse. Singular value analysis for two cases of low-pass filtering *Inverse Problems* **1** 67–85
- [6] Bertero M, De Mol C and Pike E R 1985 Linear inverse problems with discrete data. I: General formulation and singular system analysis *Inverse Problems* **1** 301–30
- [7] Luttrell S P 1985 The use of transinformation in the design of data sampling schemes for inverse problems *Inverse Problems* **1** 199–218